

# 7.2-kW, GaN-Based Single-Phase String Inverter With Battery Energy Storage System Reference Design



## Description

This reference design provides an overview into the implementation of a GaN-based single-phase string inverter with bidirectional power conversion system for Battery Energy Storage Systems (BESS). The design consists of two string inputs, each able to handle up to 10 photovoltaic (PV) panels in series and one energy storage system port that can handle battery stacks ranging from 80 V to 500 V. The rated power from string inputs to battery storage systems is up to 7.2 kW. The configurable DC-AC converter can support up to 3.6 kW into a single-phase grid connection at 230 V. Digital control of the three power stages is executed on a single C2000™ MCU.

## Resources

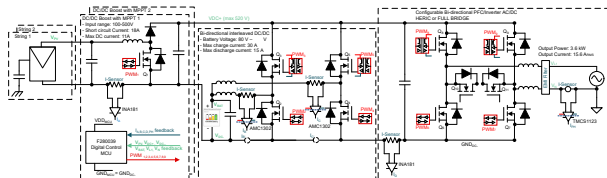
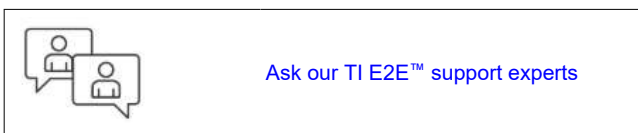
|                                       |                |
|---------------------------------------|----------------|
| <a href="#">TIDA-010938</a>           | Design Folder  |
| <a href="#">LMG3522R030, TMCS1123</a> | Product Folder |
| <a href="#">AMC1302, ISOW1044</a>     | Product Folder |
| <a href="#">ISO1412, UCC14131-Q1</a>  | Product Folder |
| <a href="#">ISO7741, ISO7762</a>      | Product Folder |
| <a href="#">OPA4388, INA181</a>       | Product Folder |
| <a href="#">TMDSNCD280039C</a>        | Product Folder |

## Features

- Bidirectional DC-DC stage configurable for wide battery voltage ranges
- Configurable DC-AC stage (HERIC, H-Bridge uni- and bi-polar modulation schemes)
- 2 × power density improvement makes solar inverters lighter and easier to install
- Low total losses (< 2%) harnesses more sun and makes battery energy storage more efficient
- Cost-optimized with MCU GND referenced to  $V_{DC-}$ , allows use of non-isolated drive on all GaN devices connected to  $V_{DC-}$

## Applications

- [String inverter](#)
- [Power conversion system \(PCS\)](#)



## 1 System Description

With an increase in demand for photovoltaic systems, inverters play an important role in facilitating the transition to renewable energy further and making solar energy more accessible for residential purposes. The modularity of string inverters, low cost-per-watt and easy amplification to attain higher power levels makes string inverters a good candidate for the single-phase market. With the additional possibility of energy storage via batteries, hybrid string inverters provide a good outlet to maximize the power utilization of the string input, and also provide an alternate pathway to supply the grid during night or low irradiance scenarios.

Such hybrid string inverters combine PV panel power point tracking with an inverter stage and bidirectional capabilities to include a battery stage, thus increasing the need for higher power density and efficiencies. This is where Gallium Nitrate (GaN) FETs can bring multiple benefits into the picture. Since GaN FETs support high switching frequencies, GaN FETs allow the EMI filter and heat sink to be smaller, making the system more compact and lighter, thus increasing the form factor of the design.

This reference design is intended to show an implementation of a two-channel single-phase string inverter with fully bidirectional power flow to combine PV input functionality with BESS supporting a wide range of battery voltages.

The design contains three main stages:

- 2 × PV input with DC-DC boost converter
- Battery input with bidirectional DC-DC converter
- DC-AC converter

This system consists of two boards that are split by different functions.

The first board, called DC-DC board, consists of two input DC-DC converters for the individual string inputs and a DC-DC converter associated with the battery stage. The second board, called DC-AC board, consists of DC-link capacitors, DC-AC converter and filtering circuits. All the high-frequency switching components in the design are based on top-side cooled GaN FETs from TI .

Both the boards are mounted above an aluminum heat sink which is connected by means of thermal interface materials to the GaN FETs. The heat sink in the design is supposed to work in static cooling condition and the size is 324 mm × 305 mm × 57 mm. Overall system dimension is 290 mm × 275 mm × 47 mm, thus leading to a volume of 3.7 liters.

## 1.1 Key System Specifications

Since this reference design is split into three main stages, the key specifications for each stage is defined individually. [Table 1-1](#) shows the key specifications for the DC-AC converter, [Table 1-2](#) for the DC-DC boost converter and [Table 1-3](#) for the bidirectional DC-DC converter.

**Table 1-1. Key System Specifications: DC-AC Stage**

| PARAMETER                          | SPECIFICATION                        |
|------------------------------------|--------------------------------------|
| Maximum   Nominal DC input voltage | 520 V   400 V                        |
| Rated output voltage               | 230 V                                |
| Rated output power                 | 3.6 kW                               |
| Switching frequency                | 100 kHz                              |
| Power factor                       | ± Active, ±Reactive                  |
| Ambient temperature range          | -40°C to +60°C                       |
| Cooling                            | Static cooling or natural convection |
| Heat sink thermal resistance       | 0.3°C/W                              |
| Total harmonic distortion (THD)    | < 5%                                 |
| DC link capacitance                | 640 µF                               |
| DC link ripple voltage             | ±22 V                                |

**Table 1-2. Key System Specifications: DC-DC Boost Stage**

| PARAMETER                           | SPECIFICATION                              |
|-------------------------------------|--|
| String input voltage                | 50 V to 500 V (up to 10 panels per string) |
| Short circuit current               | 18 A                                       |
| Nominal DC current                  | 11 A   string                              |
| Maximum   Nominal DC output voltage | 520 V   400 V                              |
| Rated output power                  | 7.2 kW                                     |
| Switching frequency                 | 120 kHz                                    |
| Ambient temperature range           | -40°C to +60°C                             |

**Table 1-3. Key System Specifications: Bidirectional DC-DC Stage**

| PARAMETER                         | SPECIFICATION   |
|-----------------------------------|-----------------|
| Maximum   Nominal DC link voltage | 520 V   400 V   |
| Charging   Discharging current    | 30 A   30 A     |
| Battery voltage range             | 80 V to 500 V   |
| Maximum output power              | 7.2 kW          |
| Switching frequency               | 60 kHz each leg |
| Ambient temperature range         | -40°C to +60°C  |



**CAUTION**

*Do not leave the design powered when unattended.*

**WARNING**

**High voltage!** Accessible high voltages are present on the board. Electric shock is possible. The board operates at voltages and currents that can cause shock, fire, or injury if not properly handled. Use the equipment with necessary caution and appropriate safeguards to avoid injuring yourself or damaging property. For safety, use of isolated test equipment with overvoltage and overcurrent protection is highly recommended.

TI considers it the user's responsibility to confirm that the voltages and isolation requirements are identified and understood before energizing the board or simulation. *When energized, do not touch the design or components connected to the design.*

**WARNING**

**Hot surface! Contact can cause burns. Do not touch!**

Some components can reach high temperatures > 55°C when the board is powered on. Do not touch the board at any point during operation or immediately after operating, as high temperatures can be present.

**WARNING**

TI intends this reference design to be operated in a **lab environment only and does not consider the design as a finished product** for general consumer use. The design is intended to be run at ambient room temperature and is not tested for operation under other ambient temperatures.

TI intends this reference design to be used only by **qualified engineers and technicians** familiar with risks associated with handling high-voltage electrical and mechanical components, systems, and subsystems.

There are **accessible high voltages present on the board**. The board operates at voltages and currents that can cause shock, fire, or injury if not properly handled or applied. Use the equipment with necessary caution and appropriate safeguards to avoid injuring yourself or damaging property.

## 2 System Overview

### 2.1 Block Diagram

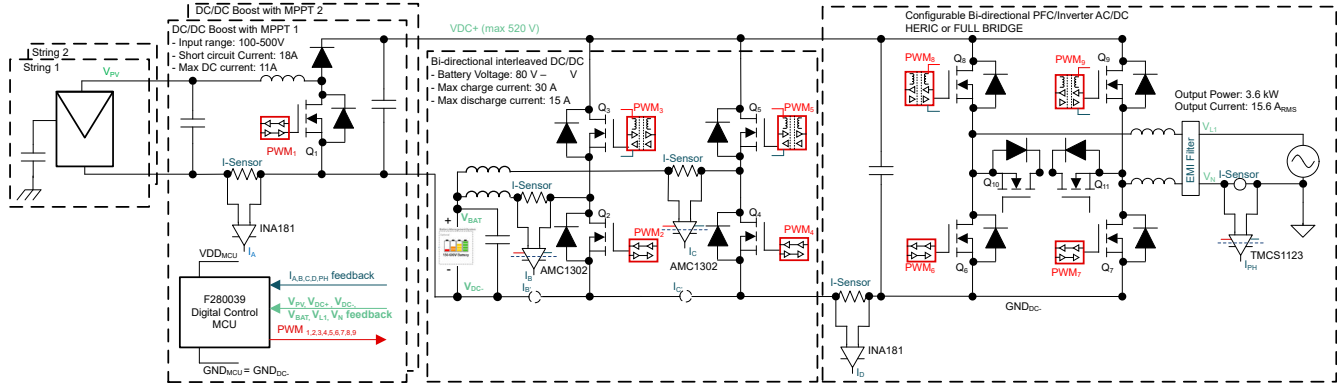


Figure 2-1. TIDA-010938 Block Diagram

### 2.2 Design Considerations

#### 2.2.1 DC-DC Boost Converter

Figure 2-2 shows a block diagram of DC-DC boost topology. This design consists of two parallel string inputs having one common output rail. Each input is connected to a DC-DC boost stage which converts the variable string output to a higher and stable DC link voltage. The stage is controlling input voltage and current and can implement Maximum Power Point Tracking (MPPT) algorithm for each string.

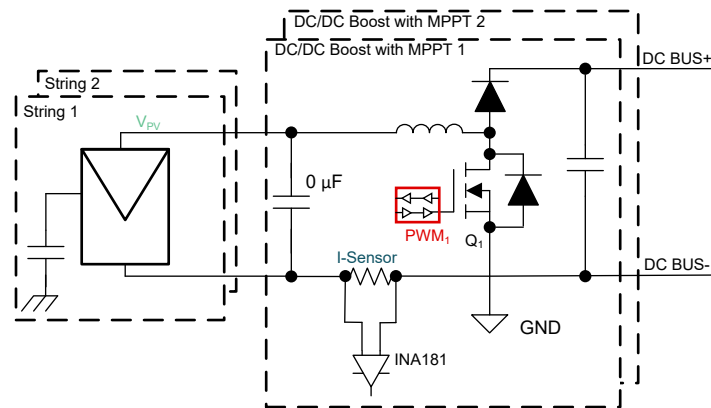


Figure 2-2. DC-DC Boost Converter Block Diagram

Each string can consist of 2 to 10 panels in series equating to an input voltage of 50 V to 500 V maximum, considering a panel is nominally 50-V rated. Both the converters are 3.6-kW rated, with an ability to provide a total output power of 7.2 kW.

The boost stages each consist of an LMG3522R030 device in combination with a SiC diode, a boost inductor 145451 (D6754) which has a value of 160  $\mu$ H, and input capacitor for filtering and a common output capacitor to minimize the output ripple voltage. By means of PLECs simulations, it was found that the LMG3522R030 30-m $\Omega$  device provides a good trade-off between conduction losses (coming from the  $R_{DS(on)}$ ) and switching losses (coming from the output parasitic capacitance). To achieve a high efficiency for the rectification stage, the SiC Schottky diode C6D20065G is used which is 650 V and 20-A rated.

In this application, the duty-cycle of the boost converter is variable and depends on the input string voltage since the DC link voltage is kept constant. The GaN FETs are switched at frequencies of 120 kHz each.

## 2.2.2 Bidirectional DC-DC Converter

Figure 2-3 shows a block diagram of the bidirectional DC-DC converter topology. In non-isolated topologies like this, a bidirectional converter can be used in systems with the possibility of battery energy storage. Bidirectionality is necessary since the converter needs to act as a battery charger (buck mode) in one direction and discharge the battery (boost mode) providing a higher and stable output voltage at the DC link.

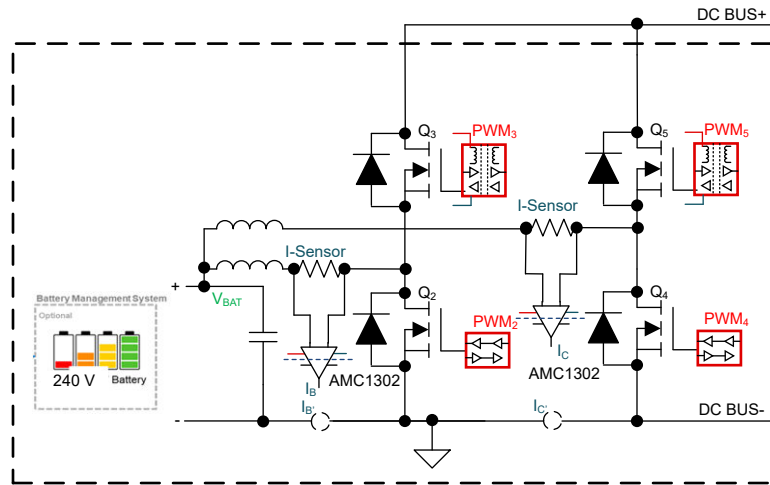


**Figure 2-3. Bidirectional DC-DC Converter Block Diagram**

In boost mode, since this converter supplies the inverter through the DC link, the discharge current is limited to 30 A. In the boost mode as well, there is a possibility to employ a charging current of 30 A to reach higher power levels. As a result, this leads to higher conduction and switching losses of the FETs, so interleaving of the branches can be carried out. Paralleling of the branches also aids in achieving twice the switching frequency across the output EMI filter which helps reduce the size. A phase difference of  $360^\circ / 2$  equals  $180^\circ$  is applied between the legs to reduce ripple current. The same current is demanded from both the branches leading to  $2 \times$  output current and the duty cycle is fixed depending on the battery voltage and the DC link voltage. Furthermore, a dead time is inserted between the half-bridge FETs to avoid short circuit of current paths, while the switches switch in a complementary fashion. Both the interleaved stages have individual input capacitor and Bourns inductor 145452 (D6755) which is  $186\text{-}\mu\text{H}$  rated, and a common output capacitor to minimize the output ripple voltage. All the passive components are designed to match the requirements for worst-case ripple and EMI conditions.

This design is therefore rated to provide a 3.6-kW output for buck stage and has a capability to charge the battery up to 7.2 kW. Each interleaved stage is switched at a frequency of 60 kHz, resulting in an equivalent output frequency of 120 kHz.

## 2.2.3 DC-AC Converter

Figure 2-4 shows a block diagram for the DC-AC stage. The inverter stage is responsible for converting DC power to AC power. The topology is constituted by an H-Bridge with each group of diagonal switches operating at high frequency during one half-wave of output voltage. Additional switches placed in parallel to the grid allows an additional voltage-level across the output filter making this power conversion system a three-level topology. This enables constant common-mode voltage leading to negligible leakage current since the PV input stage is decoupled from the AC grid in the freewheeling phase.

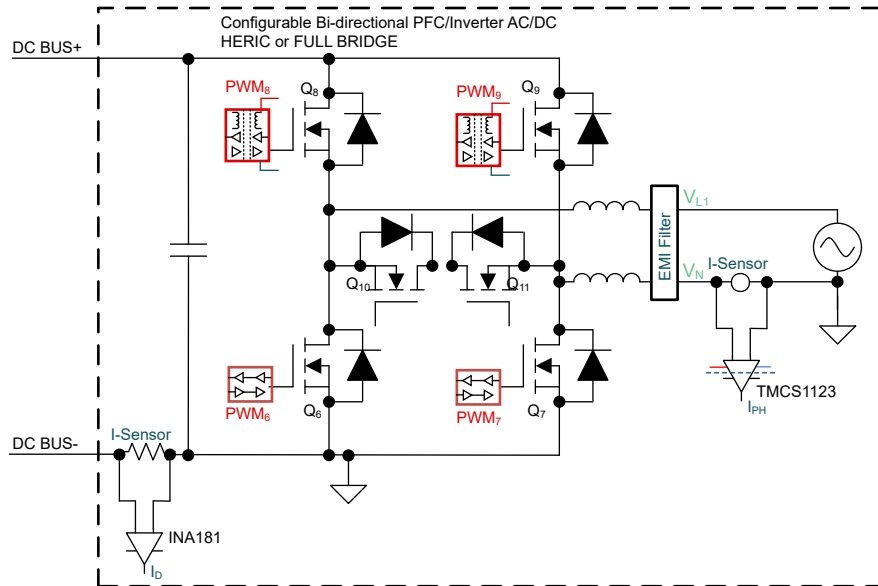


**Figure 2-4. DC-AC Converter Block Diagram**

This topology is an excellent choice for such transformerless string inverter applications where there is no isolation available between the AC grid and the PV panels. The common-mode currents are a well-known challenge in PV applications due to PV surfaces exposed over grounded roof or other surfaces in the proximity. The large surface areas can lead to high values of stray capacitance between the PV panel and ground, which can go as high as 200 nF / kWp in damp environments or on rainy days. This parasitic capacitance can cause high common-mode current flowing into the system when common-mode voltage of the converters is not well mitigated and can lead to EMI and issues such as grid current distortion.

This converter is operated at 100-kHz switching frequency for sinusoidal grid current control, allowing the EMI filter design to be compact. With the 230-V grid, an output power of 3.6 kW can be achieved with an output current of 15.6 A<sub>RMS</sub>. The EMI filter is composed of a boost inductor split between both rails, two common-mode chokes, Cx capacitors, and Cy capacitors. The EMI filter has been designed to attenuate both the differential-mode and common-mode noise injected into the grid. Additionally, electrolytic capacitors are present at the DC link to compensate for the power ripple present in such single-phase applications. For this application, the boost inductor chosen is Bourns 145453 (D6743) which is around 96 µH in value with a DC resistance of 30 mΩ. For the electrolytic capacitors, a combination of four of ALH82D161DD600 in parallel is considered, where each one is 160-µF rated leading to a total capacitance of 640 µF.

## 2.3 Highlighted Products

### 2.3.1 TMDSCNCD280039C - TMS320F280039C Evaluation Module C2000™ MCU controlCARD™

The F280039C controlCARD (TMDSCNCD280039C) from Texas Instruments (TI) provides a great way to learn and experiment with F28003x devices. The F28003x devices are members of TI's C2000™ family of microcontrollers (MCUs). This 120-pin controlCARD is intended to provide a well-filtered robust design that is capable of working in most environments.

The controlCARD™ has the following features:

- F280039C Microcontroller – High-performance C2000 microcontroller is located on the controlCARD
- 120-pin HSEC8 Edge Card Interface – Allows for compatibility with all of the 180-pin controlCARD-based application kits and controlCARDs of C2000.
- Built-in Isolated JTAG Emulation – An XDS110 emulator provides a convenient interface to Code Composer Studio™ without additional hardware. Flipping a switch allows an external JTAG emulator to be used.
- Built-in Isolated Power Supply – Passes the 5-V supply from the USB Type-C® connector through an isolation barrier. Allows for the controlCARD to be completely powered and operated from the USB Type-C connector. The F280039C is fully isolated from the USB port.
- Automatic Power Supply Switch – The controlCARD automatically switches to external 5-V power when present. No additional configuration is required.

For more details on this device, see the [TMDSCNCD280039C](#) product page.

### 2.3.2 LMG3522R030 650-V 30-mΩ GaN FET With Integrated Driver, Protection and Temperature Reporting

The LMG3522R030 GaN FET with integrated driver and protections is targeting switch-mode power converters and enables designers to achieve new levels of power density and efficiency. The LMG3522R030 integrates a silicon driver that enables switching speeds up to 150 V / ns. TI's integrated precision gate bias results in higher switching SOA compared to discrete silicon gate drivers. This integration, combined with TI's low-inductance package, delivers clean switching and minimal ringing in hard-switching power-supply topologies. Adjustable gate drive strength allows control of the slew rate from 20 V / ns to 150 V / ns, which can be used to actively control EMI and optimize switching performance. Advanced power management features include digital temperature reporting and fault detection. The temperature of the GaN FET is reported through a variable duty cycle PWM output, which simplifies managing device loading. Faults reported include overtemperature, overcurrent, and UVLO monitoring.

For more details on this device, see the [LMG3522R030](#) product page.

### 2.3.3 TMCS1123 - Precision Hall-Effect Current Sensor

The TMCS1123 is a galvanically isolated Hall-effect current sensor with industry leading isolation and accuracy. An output voltage proportional to the input current is provided with excellent linearity and low drift at all sensitivity options. Precision signal conditioning circuitry with built-in drift compensation is capable of less than 1.75% maximum total error over temperature and lifetime with no system level calibration, or less than 1% maximum total error with a one-time room temperature calibration (including both lifetime and temperature drift). AC or DC input current flows through an internal conductor generating a magnetic field measured by integrated on-chip Hall-effect sensors. Coreless construction eliminates the need for magnetic concentrators. Differential Hall sensors reject interference from stray external magnetic fields. Low conductor resistance increases measurable current ranges up to  $\pm 96$  A while minimizing power loss and easing thermal dissipation requirements. Insulation capable of withstanding 5000 V<sub>RMS</sub>, coupled with minimum 8.1-mm creepage and clearance provide up to 1100-VDC reliable lifetime reinforced working voltage. Integrated shielding enables excellent common-mode rejection and transient immunity. Fixed sensitivity allows the TMCS1123 to operate from a single 3-V to 5.5-V power supply, eliminates radiometry errors, and improves supply noise rejection.

For more details on this device, see the [TMCS1123](#) product page.

### 2.3.4 AMC1302 - Precision, $\pm 50$ -mV Input, Reinforced Isolated Amplifier

The AMC1302 is a precision, isolated amplifier with an output separated from the input circuitry by an isolation barrier that is highly resistant to magnetic interference. This barrier is certified to provide reinforced galvanic isolation of up to 5 kV<sub>RMS</sub> according to VDE V 0884-11 and UL1577, and supports a working voltage of up to 1.5

$kV_{RMS}$ . The isolation barrier separates parts of the system that operate on different common-mode voltage levels and protects the low-voltage side from hazardous voltages and damage. The input of the AMC1302 is optimized for direct connection to a low-impedance shunt resistor or other low-impedance voltage source with low signal levels. The excellent DC accuracy and low temperature drift supports accurate current control in PFC stages, DC/DC converters, AC-motor and servo drives over the extended industrial temperature range from  $-40^{\circ}\text{C}$  to  $+125^{\circ}\text{C}$ . The integrated missing-shunt and missing high-side supply detection features simplify system-level design and diagnostics.

For more details on this device, see the [AMC1302](#) product page.

### 2.3.5 ISO7741 Robust EMC, Quad-channel, 3 Forward, 1 Reverse, Reinforced Digital Isolator

The ISO7741 device is a high-performance, quad-channel digital isolator with  $5000 V_{RMS}$  (DW package) and  $3000 V_{RMS}$  (DBQ package) isolation ratings per UL 1577. The family includes devices with reinforced insulation ratings according to VDE, CSA, TUV, and CQC. The ISO7741B device is designed for applications that require basic insulation ratings only. The ISO774x devices provide high electromagnetic immunity and low emissions at low power consumption, while isolating CMOS or LVCMOS digital I/Os. Each isolation channel has a logic input and output buffer separated by a double capacitive silicon dioxide ( $\text{SiO}_2$ ) insulation barrier. These devices come with enable pins which can be used to put the respective outputs in high impedance for multi-master driving applications and to reduce power consumption. The ISO7740 device has all four channels in the same direction, the ISO7741 device has three forward channels and one reverse-direction channel, and the ISO7742 device has two forward and two reverse-direction channels.

For more details on this device, see the [ISO7741](#) product page.

### 2.3.6 ISO7762 Robust EMC, Six-Channel, 4 Forward, 2 Reverse, Reinforced Digital Isolator

The ISO7762 device is a high-performance, six-channel digital isolator with  $5000\text{-}V_{RMS}$  (DW package) and  $3000\text{-}V_{RMS}$  (DBQ package) isolation ratings per UL 1577. The family of devices is also certified according to VDE, CSA, TUV, and CQC. The ISO776x family of devices provides high electromagnetic immunity and low emissions at low-power consumption, while isolating CMOS or LVCMOS digital I/Os. Each isolation channel has a logic-input and logic-output buffer separated by a double capacitive silicon dioxide ( $\text{SiO}_2$ ) insulation barrier. The ISO776x family of devices is available in all possible pin configurations such that all six channels are in the same direction, or one, two, or three channels are in reverse direction while the remaining channels are in forward direction.

For more details on this device, see the [ISO7762](#) product page.

### 2.3.7 UCC14131-Q1 Automotive, 1.5-W, 12-V to 15-V $V_{IN}$ , 12-V to 15-V $V_{OUT}$ , High-Density > 5- $kV_{RMS}$ Isolated DC/DC Module

UCC14131-Q1 is an automotive qualified high-isolation voltage DC/DC power module designed to provide power to GaN, IGBT, SiC, or Si gate drivers. The UCC14131-Q1 integrates a transformer and DC/DC controller with a proprietary architecture to achieve high efficiency with very low emissions. The device can provide an isolated 12-V output from a 12-V regulated input for driving GaN and Si MOSFETs; and an isolated 15-V or 18-V output from a 15-V regulated input to bias the driver circuit for SiC MOSFET or IGBTs. The high-accuracy provides better channel enhancement for higher system efficiency without over-stressing the power device gate. The UCC14131-Q1 provides up to 1.5 W (typical) of isolated output power at high efficiency. Requiring a minimum of external components and including on-chip device protection, the module provides extra features such as input undervoltage lockout, overvoltage lockout, output voltage power-good comparators, overtemperature shutdown, soft-start time-out, adjustable isolated positive and negative output voltage, an enable pin, and an open-drain output power-good pin.

For more details on this device, see the [UCC14131-Q1](#) product page.

### 2.3.8 ISOW1044 Low-Emissions, 5- $kV_{RMS}$ Isolated CAN FD Transceiver With Integrated DC/DC Power

The ISOW1044 device is a galvanically-isolated controller area network (CAN) transceiver with a built-in isolated DC-DC converter that eliminates the need for a separate isolated power supply in space-constrained isolated designs. The low-emissions, isolated DC-DC meets CISPR 32 radiated emissions Class B standard with just two ferrite beads on a simple two-layer PCB. Additional 20-mA output current can be used to power other circuits on

the board. An integrated 10Mbps GPIO channel is available and can help remove an additional digital isolator or optocoupler for diagnostics, LED indication or supply monitoring.

For more details on this device, see the [ISOW1044](#) product page.

### **2.3.9 ISOW1412 Low-Emissions, 500kbps, Reinforced Isolated RS-485, RS-422 Transceiver With Integrated Power**

The ISOW1412 device is a galvanically-isolated RS-485, RS-422 transceiver with a built-in isolated DC-DC converter, that eliminates the need for a separate isolated power supply in space-constrained isolated designs. The low-emissions, isolated DC-DC converter meets CISPR 32 radiated emissions Class B standard with just two ferrite beads on a simple two-layer PCB. Additional 20-mA output current can be used to power other circuits on the board. An integrated 2Mbps GPIO channel helps remove any additional digital isolator or optocoupler for diagnostics, LED indication, or supply monitoring.

For more details on this device, see the [ISOW1412](#) product page.

### **2.3.10 OPA4388 Quad, 10-MHz, CMOS, Zero-Drift, Zero-Crossover, True RRIO Precision Operational Amplifier**

The OPA4388 precision operational amplifier is an ultra-low noise, fast-settling, zero-drift, zero-crossover device that provides rail-to-rail input and output operation. These features and excellent AC performance, combined with only 0.25  $\mu\text{V}$  of offset and 0.005  $\mu\text{V} / ^\circ\text{C}$  of drift over temperature, makes the OPA4388 a great choice for driving high-precision, analog-to digital converters (ADCs) or buffering the output of high-resolution, digital-to-analog converters (DACs). This design results in excellent performance when driving analog-to-digital converters (ADCs) without degradation of linearity. The OPA388 (single version) is available in the VSSOP-8, SOT23-5, and SOIC-8 packages. The OPA2388 (dual version) is offered in the VSSOP-8 and SO-8 packages. The OPA4388 (quad version) is offered in the TSSOP-14 and SO-14 packages. All versions are specified over the industrial temperature range of  $-40^\circ\text{C}$  to  $+125^\circ\text{C}$ .

For more details on this device, see the [OPA4388](#) product page.

### **2.3.11 OPA2388 Dual, 10-MHz, CMOS, Zero-Drift, Zero-Crossover, True RRIO Precision Operational Amplifier**

The OPA2388 is a precision operational amplifier that is an ultra-low noise, fast-settling, zero-drift, zero-crossover device that provides rail-to-rail input and output operation. These features and excellent AC performance, combined with only 0.25  $\mu\text{V}$  of offset and 0.005  $\mu\text{V} / ^\circ\text{C}$  of drift over temperature, makes the OPA2388 a great choice for driving high-precision, analog-to digital converters (ADCs) or buffering the output of high-resolution, digital-to-analog converters (DACs). This design results in excellent performance when driving analog-to-digital converters (ADCs) without degradation of linearity. The OPA388 (single version) is available in the VSSOP-8, SOT23-5, and SOIC-8 packages. The OPA2388 (dual version) is offered in the VSSOP-8 and SO-8 packages. The OPA4388 (quad version) is offered in the TSSOP-14 and SO-14 packages. All versions are specified over the industrial temperature range of  $-40^\circ\text{C}$  to  $+125^\circ\text{C}$ .

For more details on this device, see the [OPA2388](#) product page.

### **2.3.12 INA181 26-V Bidirectional 350-kHz Current-Sense Amplifier**

The INA181 is a current sense amplifier that is designed for cost-optimized applications. This device is a part of a family of bidirectional, current-sense amplifiers (also called current-shunt monitors) that sense voltage drops across current-sense resistors at common-mode voltages from  $-0.2\text{ V}$  to  $+26\text{ V}$ , independent of the supply voltage. The INAx181 family integrates a matched resistor gain network in four, fixed-gain device options: 20 V/V, 50 V/V, 100 V/V, or 200 V/V. This matched gain resistor network minimizes gain error and reduces the temperature drift. These devices operate from a single 2.7-V to 5.5-V power supply. The single-channel INA181 draws a maximum supply current of 260  $\mu\text{A}$ ; whereas, the dual-channel INA2181 draws a maximum supply current of 500  $\mu\text{A}$ , and the quad-channel INA4181 draws a maximum supply current of 900  $\mu\text{A}$ . The INA181 is available in a 6-pin, SOT-23 package. The INA2181 is available in 10-pin, VSSOP, and WSON packages. The INA4181 is available in a 20-pin, TSSOP package. All device options are specified over the extended operating temperature range of  $-40^\circ\text{C}$  to  $+125^\circ\text{C}$ .

For more details on this device, see the [INA181](#) product page.

### 3 Hardware, Software, Testing Requirements, and Test Results

#### 3.1 Hardware Requirements

The hardware for this reference design is composed of the following:

- DC-DC Board
- DC-AC Board
- TMDSCNCD280039C control card
- USB Type-C® cable
- USB isolator
- Laptop

The following test equipment is needed to power and evaluate the DUT:

- DC Power source Keysight N8950A
- DC Power source Elektro-Automatik EA-PS 3080-20C
- DC Load Chroma 63208A
- Power Analyzer Tektronix PA-4000

#### 3.2 Test Setup

The recommended sequence of tests is shown below:

1. DC-DC board with two independent DC power sources on inputs for the boost stages connecting to the DC load on the output
2. DC-DC board with DC power source on input for the bidirectional DC-DC stage connecting to the DC load on the output

##### 3.2.1 DC-DC Boost Stage

Figure 3-1 shows the connection for the boards. For safety reasons make sure that the proper voltage and current limit is selected on DC power sources. DC load needs to be configured in constant voltage mode with the required voltage and current limits. The DC bus of the DC-DC board is connected to that of the DC-AC board, and so are the connectors for the control signals. The DC load needs to be configured in constant voltage mode with the DC bus voltage of 450 V and 9-A maximum current.

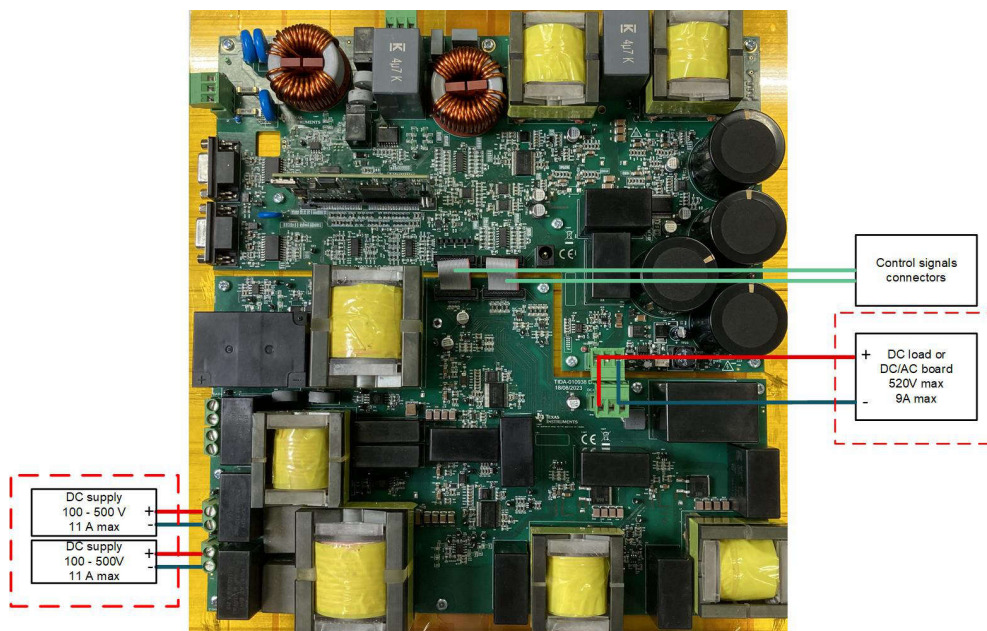


**Figure 3-1. Connections for Testing DC-DC Boost**

### 3.2.2 Bidirectional DC-DC Stage

Figure 3-2 shows the connection for the boards. For safety reasons make sure that the proper voltage and current limit is selected on DC power sources. DC load needs to be configured in constant voltage mode with the required voltage and current limits. The DC bus of the DC-DC board is connected to that of DC-AC board, and so are the connectors for the control signals. The DC load needs to be configured in constant-voltage mode with the DC bus voltage of 400 V and 20-A maximum current.

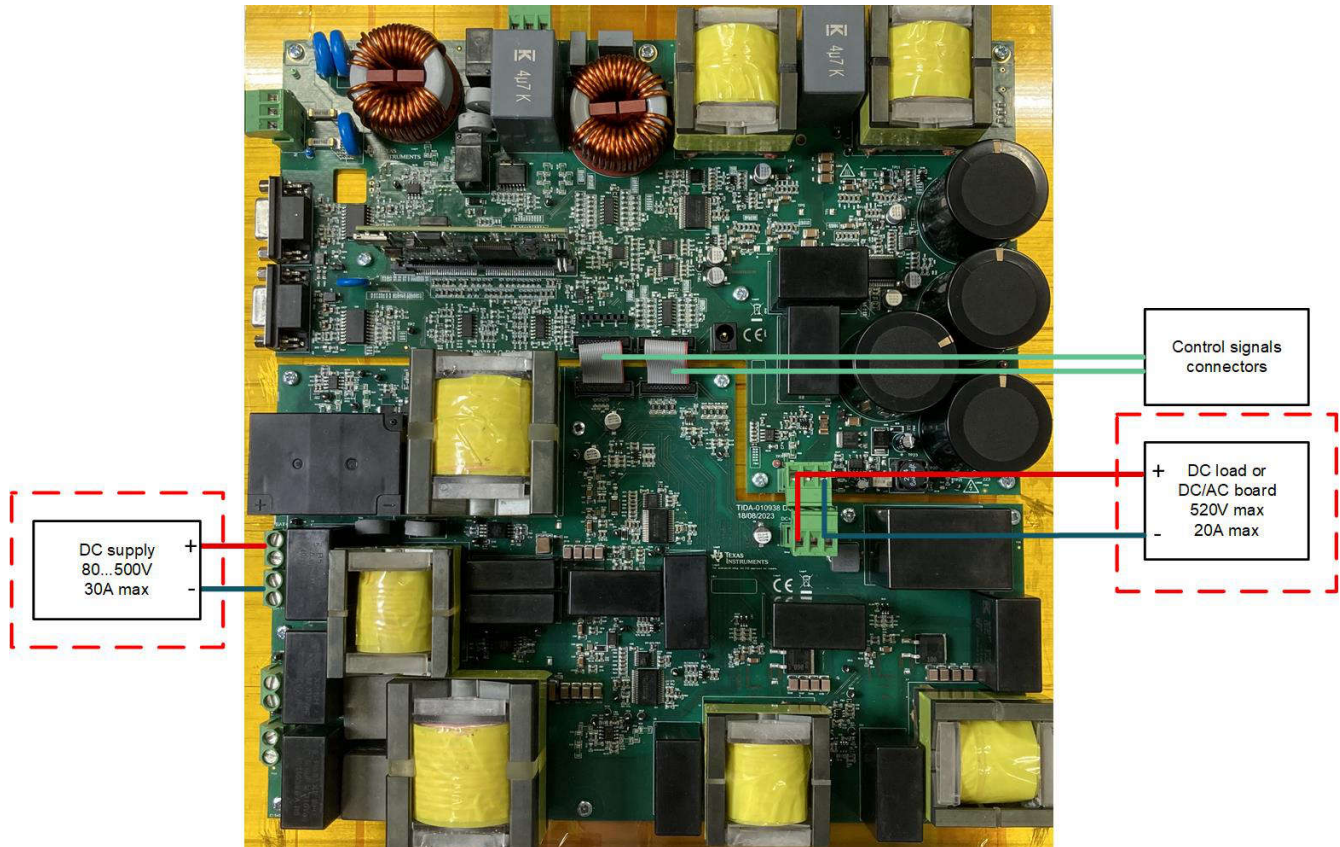


**Figure 3-2. Connections for Testing Bidirectional DC-DC**

## 3.3 Test Results

### 3.3.1 DC-DC Boost Converter

Figure 3-3 and Table 3-1 show the efficiency of input DC-DC converter at 450-V DC bus output. The input voltages considered are 225 V, 350 V, and 400 V. For 225-V input, the peak efficiency achieved is 98.8%, where the boost converter demonstrates the worst-case ripple conditions for a duty cycle of 0.5. The table shows that the converter achieves a peak efficiency of 99.3% at full load.

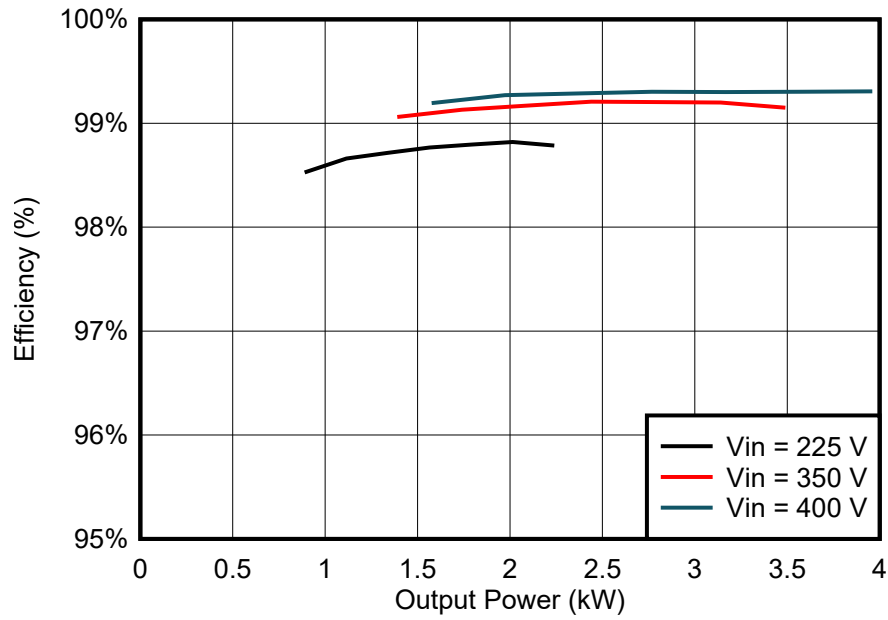


Figure 3-3. DC-DC Boost Efficiency vs Output Power at 450-V DC-Link

Table 3-1. DC-DC Boost Efficiency

| OUTPUT POWER | EFFICIENCY AT $V_{IN} = 225\text{ V}$ | OUTPUT POWER | EFFICIENCY AT $V_{IN} = 350\text{ V}$ | OUTPUT POWER | EFFICIENCY AT $V_{IN} = 400\text{ V}$ |
|--------------|---------------------------------------|--------------|---------------------------------------|--------------|---------------------------------------|
| 0.9 kW       | 98.5%                                 | 1.4 kW       | 99.0%                                 | 1.6 kW       | 99.2%                                 |
| 1.1 kW       | 98.6%                                 | 1.7 kW       | 99.1%                                 | 2.0 kW       | 99.3%                                 |
| 1.3 kW       | 98.7%                                 | 2.1 kW       | 99.2%                                 | 2.4 kW       | 99.3%                                 |
| 1.6 kW       | 98.8%                                 | 2.4 kW       | 99.2%                                 | 2.8 kW       | 99.3%                                 |
| 1.8 kW       | 98.8%                                 | 2.8 kW       | 99.2%                                 | 3.2 kW       | 99.3%                                 |
| 2.0 kW       | 98.8%                                 | 3.1 kW       | 99.2%                                 | 3.6 kW       | 99.3%                                 |
| 2.2 kW       | 98.8%                                 | 3.5 kW       | 99.1%                                 | 4.0 kW       | 99.3%                                 |

### 3.3.2 Bidirectional DC-DC Converter

Figure 3-4 and Table 3-2 show the efficiency of the bidirectional DC-DC converter functioning in buck mode at 400-V DC bus output. The input battery voltages considered are 80 V, 160 V, 240 V, and 320 V and the table shows that the converter achieves peak efficiencies of 97.9%, 99.0%, 99.2%, and 99.4% respectively.

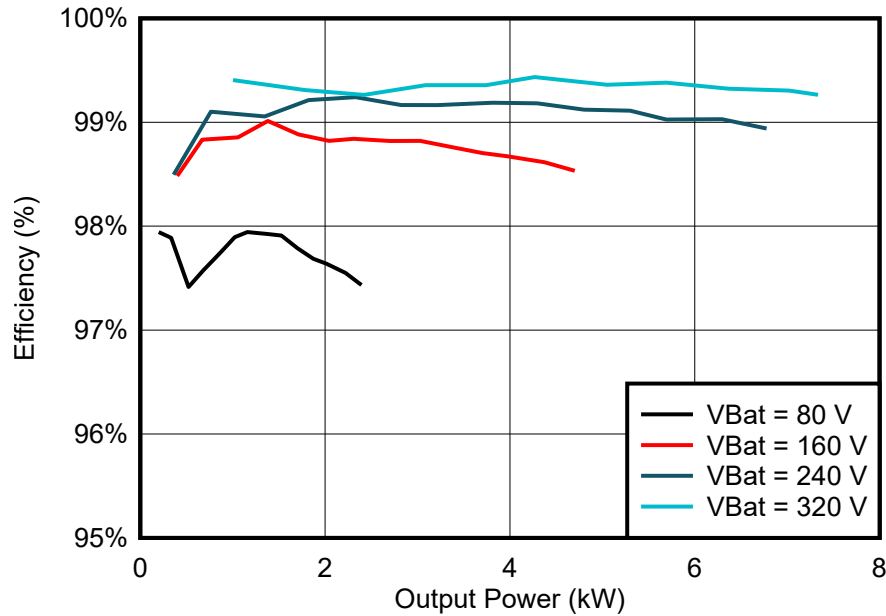
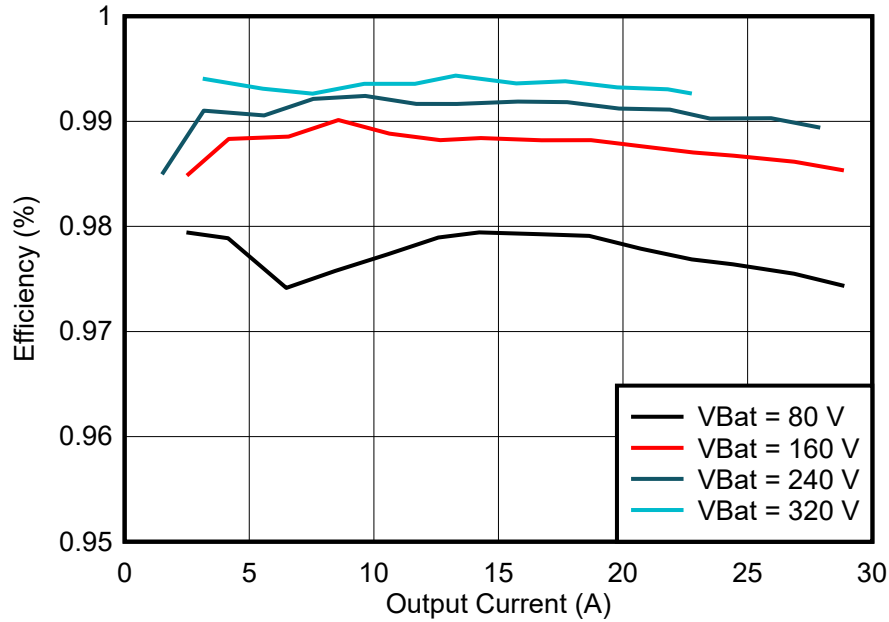


Figure 3-4. Bidirectional DC-DC Efficiency vs Output Power at 400-V DC-Link

Table 3-2. Bidirectional DC-DC Efficiency

| OUTPUT POWER | EFFICIENCY AT VBat = 80 V | OUTPUT POWER | EFFICIENCY AT VBat = 160 V | OUTPUT POWER | EFFICIENCY AT VBat = 240 V | OUTPUT POWER | EFFICIENCY AT VBat = 320 V |
|--------------|---------------------------|--------------|----------------------------|--------------|----------------------------|--------------|----------------------------|
| 0.2 kW       | 97.9%                     | 0.4 kW       | 98.5%                      | 0.4 kW       | 98.5%                      | 1.0 kW       | 99.4%                      |
| 0.3 kW       | 97.9%                     | 0.7 kW       | 98.8%                      | 0.8 kW       | 99.1%                      | 1.8 kW       | 99.3%                      |
| 0.5 kW       | 97.4%                     | 1.1 kW       | 98.9%                      | 1.3 kW       | 99.1%                      | 2.4 kW       | 99.3%                      |
| 0.7 kW       | 97.6%                     | 1.4 kW       | 99.0%                      | 1.8 kW       | 99.2%                      | 3.1 kW       | 99.4%                      |
| 0.9 kW       | 97.7%                     | 1.7 kW       | 98.9%                      | 2.3 kW       | 99.2%                      | 3.7 kW       | 99.4%                      |
| 1.0 kW       | 97.9%                     | 2.0 kW       | 98.8%                      | 2.8 kW       | 99.2%                      | 4.3 kW       | 99.4%                      |
| 1.2 kW       | 97.9%                     | 2.3 kW       | 98.8%                      | 3.2 kW       | 99.2%                      | 5.1 kW       | 99.4%                      |
| 1.4 kW       | 97.9%                     | 2.7 kW       | 98.8%                      | 3.8 kW       | 99.2%                      | 5.7 kW       | 99.4%                      |
| 1.5 kW       | 97.9%                     | 3.0 kW       | 98.8%                      | 4.3 kW       | 99.2%                      | 6.4 kW       | 99.3%                      |
| 1.7 kW       | 97.8%                     | 3.4 kW       | 98.8%                      | 4.8 kW       | 99.1%                      | 7.0 kW       | 99.3%                      |
| 1.9 kW       | 97.7%                     | 3.7 kW       | 98.7%                      | 5.3 kW       | 99.1%                      | 7.3 kW       | 99.3%                      |
| 2.0 kW       | 97.6%                     | 4.0 kW       | 98.7%                      | 5.7 kW       | 99.0%                      |              |                            |
| 2.2 kW       | 97.6%                     | 4.4 kW       | 98.6%                      | 6.3 kW       | 99.0%                      |              |                            |
| 2.4 kW       | 97.4%                     | 4.7 kW       | 98.5%                      | 6.8 kW       | 98.9%                      |              |                            |

Figure 3-5 and Table 3-3 further show the efficiency of this converter versus output current at 400-V DC bus to demonstrate the capability in handling currents up to 30 A.



**Figure 3-5. Bidirectional DC-DC Converter Efficiency vs Output Current at 400-V DC-Link**

**Table 3-3. Bidirectional DC-DC Converter**

| OUTPUT CURRENT | EFFICIENCY AT VBat = 80 V | OUTPUT CURRENT | EFFICIENCY AT VBat = 160 V | OUTPUT CURRENT | EFFICIENCY AT VBat = 240 V | OUTPUT CURRENT | VBat = 320 V |
|----------------|---------------------------|----------------|----------------------------|----------------|----------------------------|----------------|--------------|
| 2.5 A          | 97.9%                     | 2.5 A          | 98.5%                      | 1.5 A          | 98.5%                      | 3.1 A          | 99.4%        |
| 4.1 A          | 97.9%                     | 4.2 A          | 98.8%                      | 3.2 A          | 99.1%                      | 5.6 A          | 99.3%        |
| 6.5 A          | 97.4%                     | 6.6 A          | 98.9%                      | 5.6 A          | 99.1%                      | 7.5 A          | 99.3%        |
| 8.5 A          | 97.6%                     | 8.6 A          | 99.0%                      | 7.6 A          | 99.2%                      | 9.6 A          | 99.4%        |
| 10.6 A         | 97.7%                     | 10.6 A         | 98.9%                      | 9.7 A          | 99.2%                      | 11.7 A         | 99.4%        |
| 12.6 A         | 97.9%                     | 12.7 A         | 98.8%                      | 11.7 A         | 99.2%                      | 13.3 A         | 99.4%        |
| 14.2 A         | 97.9%                     | 14.3 A         | 98.8%                      | 13.3 A         | 99.2%                      | 15.7 A         | 99.4%        |
| 16.7 A         | 97.9%                     | 16.7 A         | 98.8%                      | 15.8 A         | 99.2%                      | 17.7 A         | 99.4%        |
| 18.6 A         | 97.9%                     | 18.7 A         | 98.8%                      | 17.8 A         | 99.2%                      | 19.8 A         | 99.3%        |
| 20.7 A         | 97.8%                     | 20.8 A         | 98.8%                      | 19.8 A         | 99.1%                      | 21.8 A         | 99.3%        |
| 22.8 A         | 97.7%                     | 22.8 A         | 98.7%                      | 21.9 A         | 99.1%                      | 22.8 A         | 99.3%        |
| 24.4 A         | 97.6%                     | 24.4 A         | 98.7%                      | 23.5 A         | 99.0%                      |                |              |
| 26.9 A         | 97.6%                     | 26.9 A         | 98.6%                      | 25.9 A         | 99.0%                      |                |              |
| 28.9 A         | 97.4%                     | 28.9 A         | 98.5%                      | 27.9 A         | 99.0%                      |                |              |

## 4 Design and Documentation Support

### 4.1 Design Files

#### 4.1.1 Schematics

To download the schematics, see the design files at [TIDA-010938](#).

#### 4.1.2 BOM

To download the bill of materials (BOM), see the design files at [TIDA-010938](#).

### 4.2 Tools and Software

#### Tools

[TMDSCNCD280039C](#) TMS320F280039C evaluation module C2000™ MCU controlCARD™

#### Software

[Code Composer Studio™](#) Integrated development environment (IDE)

### 4.3 Documentation Support

1. Texas Instruments, [TMS320F280039C controlCARD Information Guide](#) user's guide

### 4.4 Support Resources

[TI E2E™ support forums](#) are an engineer's go-to source for fast, verified answers and design help — straight from the experts. Search existing answers or ask your own question to get the quick design help you need.

Linked content is provided "AS IS" by the respective contributors. They do not constitute TI specifications and do not necessarily reflect TI's views; see TI's [Terms of Use](#).

### 4.5 Trademarks

C2000™, TI E2E™, and Code Composer Studio™, and are trademarks of Texas Instruments.

USB Type-C® is a registered trademark of USB Implementers Forum.

All trademarks are the property of their respective owners.

## 5 About the Author

**VEDATROYEE GHOSH** is a Systems Engineer at Texas Instruments Germany, where she focuses on solar energy within the Grid Infrastructure team. Vedatroyee has earned her master's degree in Power Engineering from the Technical University of Munich, Germany, in 2023.

**RICCARDO RUFFO** received the Ph.D. degree in Electric, Electronics and Communication Engineering from Politecnico di Torino, Turin, Italy, in 2019. He is currently working at Texas Instruments Germany as System Engineer in the area of Grid Infrastructure, Renewable Energy. His main work includes EV charging, inductive wireless power transfer, photovoltaic, renewable energy, and energy storage applications.

**ANDREAS LECHNER** is a Systems Engineer for Grid Infrastructure working in Texas Instruments. Andreas is supporting customers within the Grid Infrastructure sector worldwide. Andreas earned his master's degree from the University of Applied Sciences in Landshut, Germany.

**VSEVOLOD ELANTSEV** is a Systems Engineer for Grid Infrastructure in Texas Instruments Germany. Vsevolod is focusing on power conversion systems. Vsevolod graduated from the South Russian State Technical University, Novocherkassk, Russia, in 2011.

## IMPORTANT NOTICE AND DISCLAIMER

TI PROVIDES TECHNICAL AND RELIABILITY DATA (INCLUDING DATA SHEETS), DESIGN RESOURCES (INCLUDING REFERENCE DESIGNS), APPLICATION OR OTHER DESIGN ADVICE, WEB TOOLS, SAFETY INFORMATION, AND OTHER RESOURCES "AS IS" AND WITH ALL FAULTS, AND DISCLAIMS ALL WARRANTIES, EXPRESS AND IMPLIED, INCLUDING WITHOUT LIMITATION ANY IMPLIED WARRANTIES OF MERCHANTABILITY, FITNESS FOR A PARTICULAR PURPOSE OR NON-INFRINGEMENT OF THIRD PARTY INTELLECTUAL PROPERTY RIGHTS.

These resources are intended for skilled developers designing with TI products. You are solely responsible for (1) selecting the appropriate TI products for your application, (2) designing, validating and testing your application, and (3) ensuring your application meets applicable standards, and any other safety, security, regulatory or other requirements.

These resources are subject to change without notice. TI grants you permission to use these resources only for development of an application that uses the TI products described in the resource. Other reproduction and display of these resources is prohibited. No license is granted to any other TI intellectual property right or to any third party intellectual property right. TI disclaims responsibility for, and you will fully indemnify TI and its representatives against, any claims, damages, costs, losses, and liabilities arising out of your use of these resources.

TI's products are provided subject to [TI's Terms of Sale](#) or other applicable terms available either on [ti.com](https://www.ti.com) or provided in conjunction with such TI products. TI's provision of these resources does not expand or otherwise alter TI's applicable warranties or warranty disclaimers for TI products.

TI objects to and rejects any additional or different terms you may have proposed.

Mailing Address: Texas Instruments, Post Office Box 655303, Dallas, Texas 75265  
Copyright © 2023, Texas Instruments Incorporated